

Supporting Information

Highly Efficient Luminescent Benzoylimino Derivative and Fluorescent Probe for Oxygen Sensor from a Photo-Chemical Reaction of Imidazole

Yue Yu,^a Ruiyang Zhao,^b Changjiang Zhou,^c Xiaoyi Sun,^c Shizhao Wang,^a Yu Gao,^c Weijun Li,^{*,a} Ping Lu,^c Bing Yang^c and Cheng Zhang^{*,a}

a. State Key Laboratory Breeding Base of Green Chemistry Synthesis Technology, College of Chemical Engineering, Zhejiang University of Technology, Hangzhou 310014, P.R. China. E-mail: liwj@zjut.edu.cn; czhang@zjut.edu.cn

b. College of Chemical Engineering, Qingdao University of Science and Technology, Qingdao, 266042, P. R. China

c. State Key Lab of Supramolecular Structure and Materials, Jilin University, 2699 Qianjin Avenue, Changchun 130012, P.R. China

Contents

- 1. Materials and character**
- 2. Synthesis**
- 3. Photoelectric properties**
- 4. Theoretical calculations**

1. Materials and character

All of the reagents and solvents used for the syntheses were purchased from Energy were used without further purification. All of the reactions were performed under a dry-nitrogen atmosphere. The ^1H NMR spectra were recorded on Bruker AVANCE III instrument (Bruker, Switzerland) by utilizing deuterated dimethyl sulfoxide (DMSO) or toluene- d_8 as solvents and tetramethylsilane (TMS) as a standard. The MALDI-TOF-MS mass spectra were recorded using an AXIMA-CFRM plus instrument. The compounds were characterized by a Vario MICRO cube elemental analyzer instrument (German Elementar Company). UV-vis absorption spectra were recorded on a UV-1800 spectrophotometer. Fluorescence measurements were carried out with a HORIBA fluorolog-3 instrument. The spin trapping-ESR tests were carried out with Bruker A300-10/12 electron paramagnetic resonance. The PL spectra in the NIR range and the lifetime measurement were carried out in a FLS980 Spectrometer with the InGaAs PDA NIR detector. X-ray diffraction was carried out with a X'Pert Pro instrument. Spin coating was carried out with WS-650MZ-8NPPB spin coater. The single crystal structure was carried out with a Agilent Geminie instrument. The differential scanning calorimetry (DSC) analysis was determined using a NETZSCH (DSC-204) instrument at $10\text{ }^\circ\text{C min}^{-1}$ under nitrogen flushing. The UV light we used in the photochemical reaction is the common ZF-7 portable UV light (6w, 365nm). The EL devices were fabricated by vacuum deposition of the materials at 10^{-6} Torr onto ITO glass with a sheet resistance of $25\ \Omega\ \text{square}^{-1}$. All of the organic layers were deposited at a rate of $1.0\ \text{Å s}^{-1}$. The cathode was deposited with LiF (1 nm) at a deposition rate of $0.1\ \text{Å s}^{-1}$ and then capping with Al metal (100 nm) through thermal evaporation at a rate of $4.0\ \text{Å s}^{-1}$. The luminance-current and density-voltage characteristics were recorded simultaneously with the measurement of the EL spectra by combining the PR650 spectrometer with a Keithley model 2400 programmable voltage-current source. All measurements were carried out at room temperature under ambient conditions.

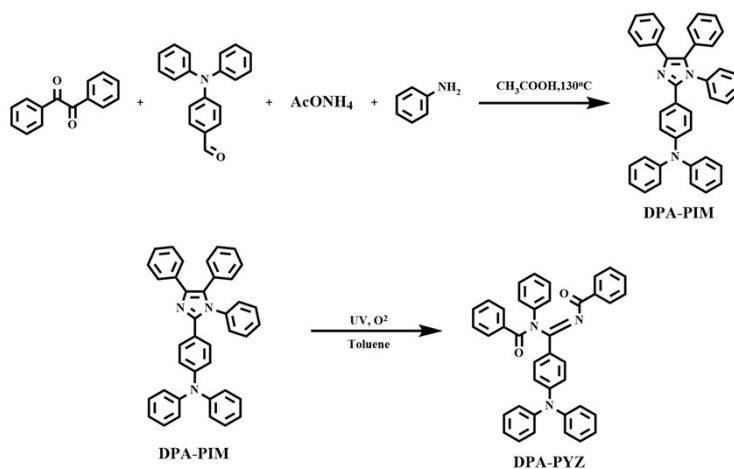
Spin Trapping-ESR Tests for the singlet oxygen $^1\text{O}_2$: 0.5 mg/ml toluene solution of sample was dispersed by ultrasonic for 30min, got 100ul of this solution mixed with 10 ppm 2,2,6,6-Tetramethylpiperidinoxy (TEMPO); after being illuminated for 10min (365nm), the mixture was characterized using a Bruker A300 ESR spectrometer. The superoxide anion radical $\text{O}_2^{\cdot-}$ trapping-ESR tests were also performed as described above, except the use of 5,5-dimethyl-1-pyrroline *N*-oxide (DMPO) as the spin-trapping agent. The feature of the signal about singlet oxygen was a triplet 1:1:1 peak with the nearly equal intensity. The description of featured triplet signals of singlet oxygen could be found in many other literatures^[1]. As for the superoxide anion radical, the feature of the signal is a quartet peak, whose relative peak intensity differs from that of hydroxyl radical (the quartet 1:2:2:1 peak) and may vary little in the relative intensity of peaks during the different testing environment. The description of featured quartet signals of superoxide anion radical could also be found in many literatures^[2]. About oxygen detector: the ratio of N_2 and O_2 were controlled by speed of gas flow respectively which was adjusted by flowmeter. N_2 and O_2 were thorough mixed until stable in a big container before measurement. And the speed of gas flow for N_2 and O_2 were controlled to be 500/1, 100/1, 100/2 ml/min respectively to get the ratio about 0.2%, 1%, 2%. The film of DPA-PIM was prepared by spin coating the 5mg/ml dichloromethane solution, the spin speed was 1000 rpm, and spin time was 60 seconds. PL spectra measurement for oxygen detection was carried out with HORIBA fluorolog-3 instrument, the excitation wavelength was 350nm, the emission wavelength was 370nm to 680nm, the slit was 5nm, and the integration time was 0.5s. The irradiation was all come from excitation light source, and thus the duration of irradiation for every measurement was about 155 seconds.

2. Synthesis

Synthesis of N,N-diphenyl-4-(1,4,5-triphenyl-1H-imidazol-2-yl)aniline (DPA-PIM): A mixture of aniline (931mg, 10.0 mmol), benzil (420mg, 2.0 mmol), 4-(N,N-Diphenylamino)benzaldehyde (546mg, 2.0 mmol), ammonium acetate (617mg, 8.0 mmol), and acetic acid (15 mL) was stirred at 120°C for 14h under nitrogen, Then, 100ml water was added to the resulting solution and the mixture was extracted with chloroform several times. The organic phase was dried over anhydrous magnesium sulfate. After filtration and solvent evaporation, the liquid was purified by column chromatography using petroleum ether/ CH_2Cl_2 as the eluent to afford a white solid (916 mg, 85%). ^1H NMR (500 MHz, Tol) δ 8.07 – 8.02 (m, 2H), 7.57 – 7.51 (m, 2H), 7.19 (t, $J = 7.7$ Hz, 2H), 7.09 – 7.03 (m, 2H), 6.99 (dd, $J = 4.2, 2.9$ Hz, 8H), 6.92 (ddd, $J = 6.2, 5.8, 2.2$ Hz, 5H), 6.90 – 6.82 (m, 1H), 6.83 – 6.72 (m, 7H). MS (ESI): MW 539.68, m/z 541.8 (M+). Anal. Calcd for $\text{C}_{39}\text{H}_{29}\text{N}_3$: C, 86.80; H, 5.42; N, 7.79; Found: C, 86.54; H, 5.49; N, 7.66.

Preparation of DPA-PYZ: DPA-PIM (500mg, 0.92mmol) is dissolved in toluene and irradiated by 365nm UV lamp for about 24h.

After evaporation, the resulting solution was purified by column chromatography using ethyl acetate/petroleum ether as the eluent to afford the product as an orange solid (350mg, 67%). $^1\text{H NMR}$ (500 MHz, Tol) δ 7.97 – 7.85 (m, 4H), 7.66 (d, J = 8.8 Hz, 2H), 7.31 – 7.19 (m, 3H), 7.16 (d, J = 4.2 Hz, 1H), 7.04 (s, 2H), 6.99 – 6.85 (m, 12H), 6.82 (t, J = 7.9 Hz, 2H), 6.75 (d, J = 8.8 Hz, 2H), 6.66 (t, J = 7.5 Hz, 1H). MS (ESI): MW 571.6, m/z 573.6 (M^+). Anal. Calcd for $\text{C}_{39}\text{H}_{29}\text{N}_3\text{O}_2$: C, 81.94; H, 5.11; N, 7.35; Found: C, 81.68; H, 5.29; N, 7.15.



Scheme S1. The synthesis of DPA-PIM and DPA-PYZ

3. Photoelectric properties.

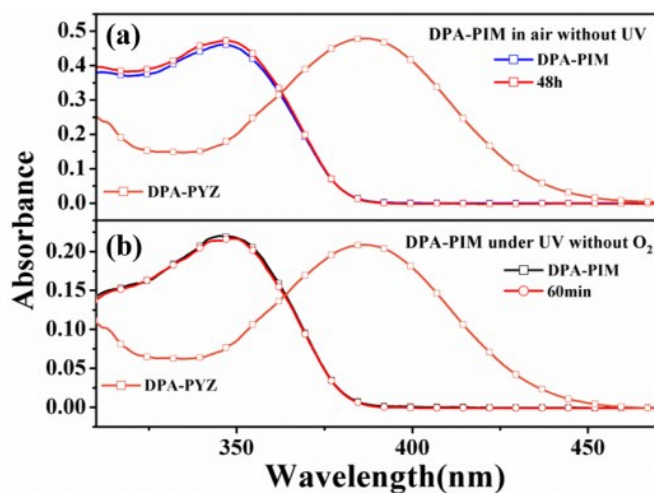


Figure S1. In-situ absorption spectra of DPA-PIM in toluene solvent at 10^{-5} mol L^{-1} with that of DPA-PYZ as reference. (a) in air (O_2) for long time of about 2 days without UV irradiation (365 nm) (b) under the UV irradiation in the N_2 atmosphere with the absence of O_2 .

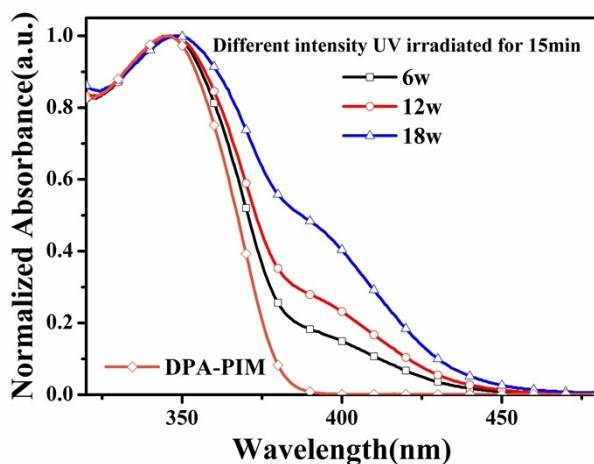


Figure S2. Absorption spectra of DPA-PIM in toluene solvent at 10^{-5} mol L^{-1} after UV irradiation by different intensity 365nm UV lamp (6w, 12w, 18w) in air for the same 15min with that of DPA-PIM before irradiated as reference.

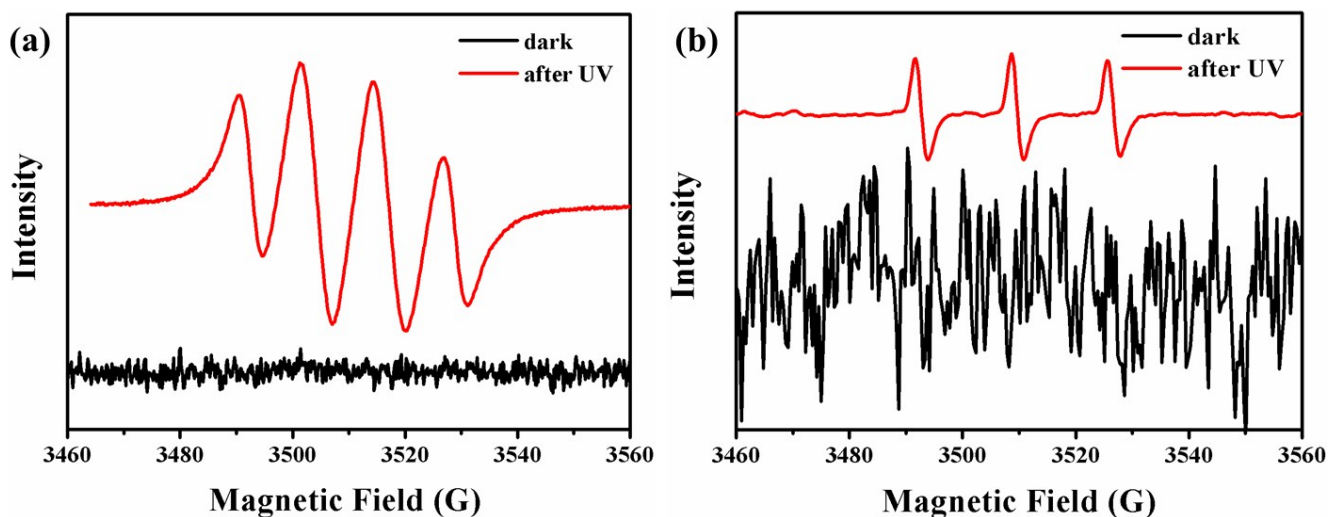


Figure S3. ESR spectra of 100ul 0.5 mg/ml DPA-PIM solution in toluene with a) 10ppm DMPO as well as b) 10ppm TEMPO a before and after 365nm UV irradiation for 10min.

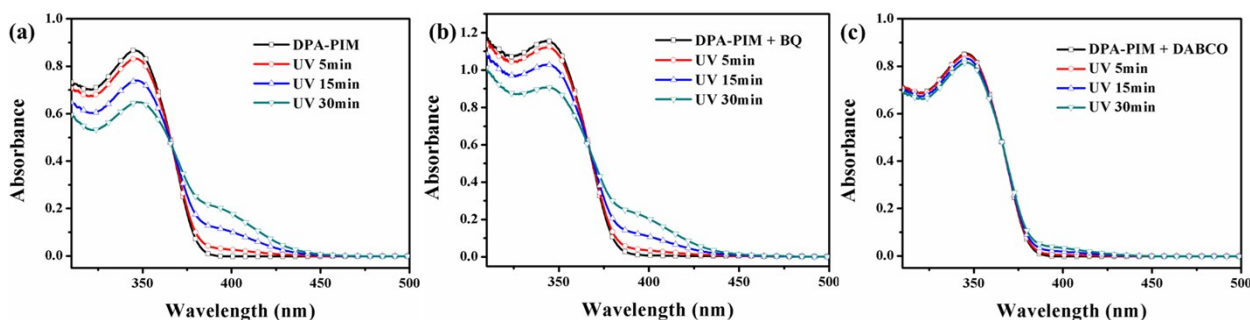


Figure 4. Absorption spectra of a) DPA-PIM, b) DPA-PIM with 10-fold BQ, and c) DPA-PIM with 20-fold DABCO in toluene solvent at 10^{-5} mol L^{-1} after UV irradiation by UV lamp in air for different time.

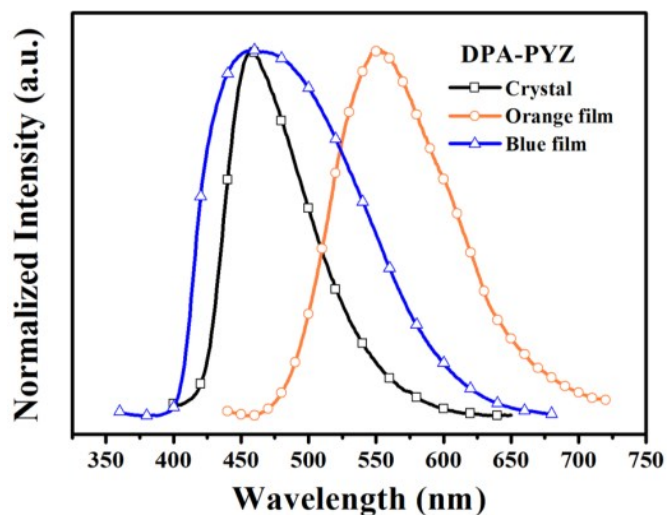


Figure S5. PL spectra of DPA-PYZ orange film (spin-coated), DPA-PYZ blue film, DPA-PYZ crystal. (The yellow-emitted film of DPA-PYZ was prepared by spin coating the 5 mg/ml dichloromethane solution. The spin speed was 1000 rpm, spin time was 60 seconds. The blue-emitted film could be obtained from the prepared yellow-emitted film by heating at about 60°C on hot planes for hours or long-time shelving at room temperature for two or more days.)

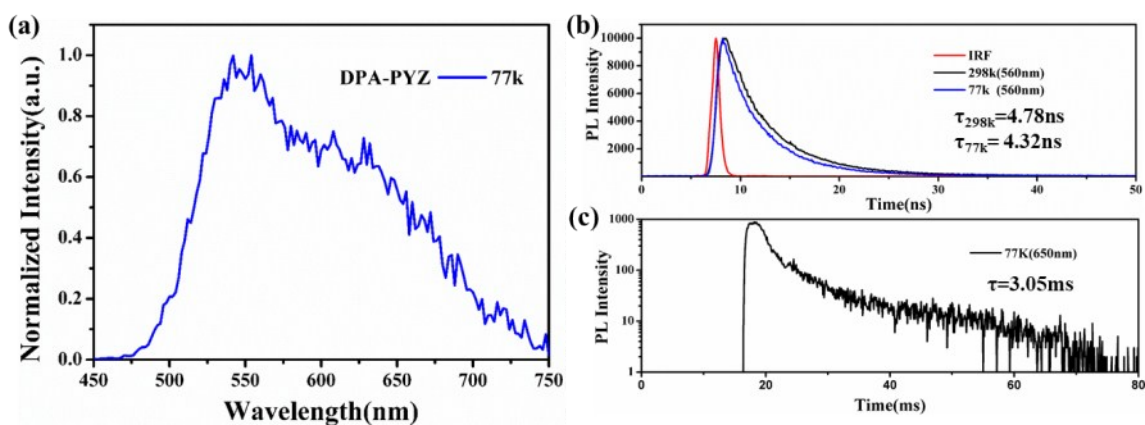


Figure S6. a) The PL spectra of spin-coated DPA-PYZ film under 77K; b) lifetime measurement of DPA-PYZ film at 560nm under 77K and at room temperature (298K, in vacuum); c) lifetime measurement of DPA-PYZ film at 650nm under 77K.

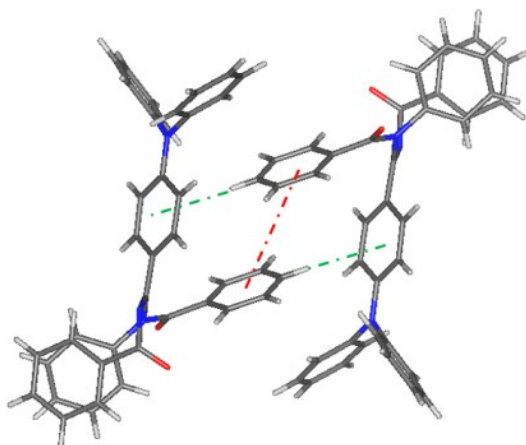


Figure S7. Packing modes of DPA-PYZ in the crystal.

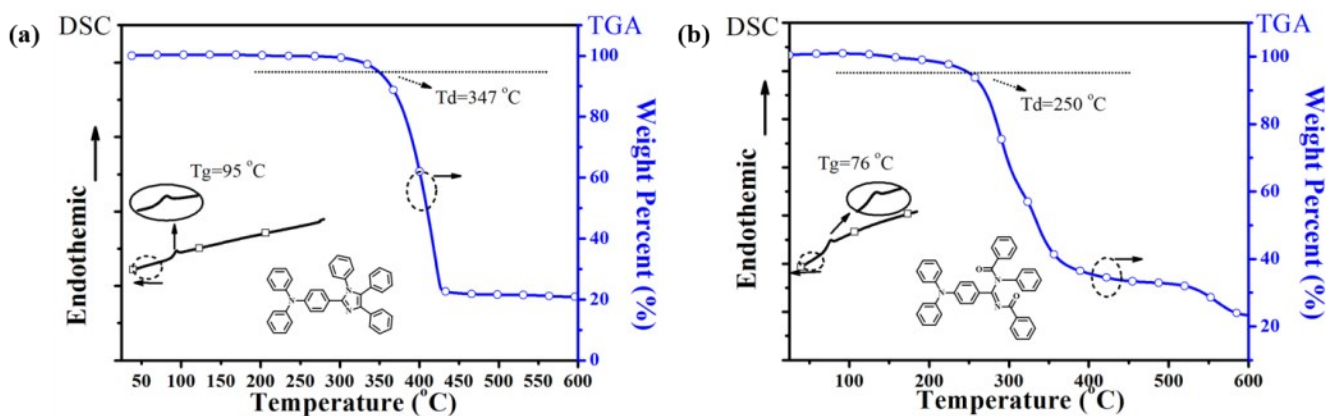


Figure S8. The DSC and TGA graphs of (a) DPA-PIM and (b) DPA-PYZ

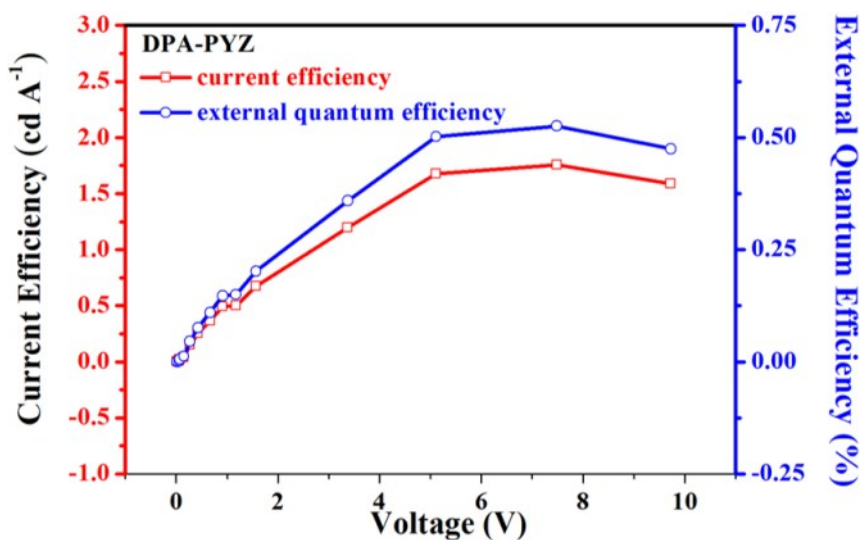


Figure S9. The Current efficiency–voltage–external quantum efficiency curve of a multilayered OLED based on DPA-PYZ as the emitter with device structures of ITO/PEDOT:PSS(40nm)/DPA-PYZ(50nm)/TPBi(30nm)/LiF/Al in which the DPA-PYZ layer was prepared by spin-coated method.

4. Theoretical calculations

The molecular geometries were optimized by Time dependent density functional theory (TD-DFT) with the CAM-B3LYP functional at the level of 6-31G* basis set. The isovalue was set to be 0.02. The xyz coordinates and the list of energies of frontier energy levels were shown in Table S1 and S2 respectively, which indicated none existence of degenerate levels.

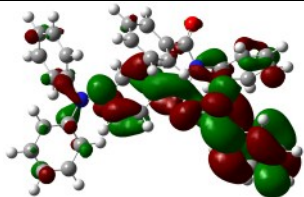
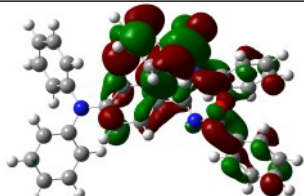
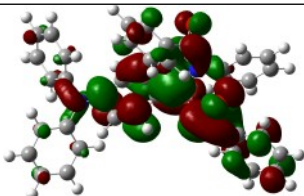
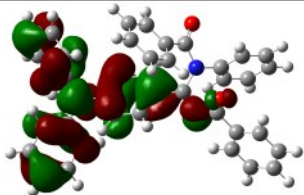
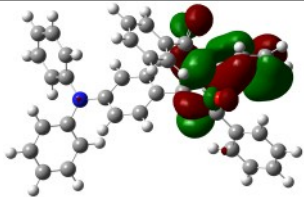
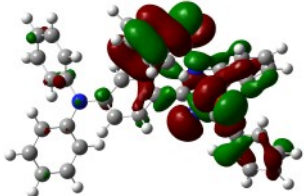
Table S1. The coordinates in optimized DPA-PYZ molecule

atom	x	y	z
N	4.053201	-0.71423	0.258986
C	2.664574	-0.52001	0.154791
O	-3.97119	0.238206	-1.88686
O	-1.82262	3.369007	1.132024
C	-0.12663	-0.10214	-0.07708
C	-1.58618	0.068892	-0.20117

C	1.920644	-1.15017	-0.86609
H	2.428574	-1.78446	-1.58325
C	0.554973	-0.94977	-0.969
H	-0.00815	-1.43145	-1.76086
N	-2.28785	-0.85359	-0.75987
N	-2.16581	1.218737	0.414337
C	1.98134	0.310504	1.064049
H	2.527591	0.784738	1.870938
C	0.615044	0.519625	0.942215
H	0.115405	1.153921	1.666935
C	-3.6105	-0.69798	-1.17739
C	4.650716	-1.94305	-0.15361
C	4.896587	0.315022	0.776012
C	-1.64155	2.526273	0.268021
C	-4.53357	-1.81449	-0.81606
C	-3.26037	1.025291	1.329263
C	-0.92353	2.849616	-1.0043
C	4.105878	-3.17121	0.249721
H	3.221191	-3.18186	0.877713
C	-1.32224	2.32738	-2.24342
H	-2.15876	1.636389	-2.30219
C	5.883252	0.005974	1.723206
H	5.987439	-1.01712	2.068731
C	-4.09016	-2.94483	-0.11602
H	-3.04267	-3.02072	0.154459
C	4.761594	1.638764	0.33099
H	4.004431	1.880053	-0.40777
C	0.106513	3.799867	-0.94562
H	0.374234	4.22156	0.017458
C	-5.88166	-1.71383	-1.18771
H	-6.20269	-0.83148	-1.73064
C	5.593243	2.634748	0.83925
H	5.477847	3.655766	0.487449
C	6.721734	1.005822	2.212621
H	7.481509	0.752579	2.94621
C	5.802521	-1.93254	-0.95358
H	6.224181	-0.98347	-1.26743
C	0.763641	4.191449	-2.10778
H	1.569394	4.917971	-2.05638
C	0.376552	3.659316	-3.34164
H	0.883885	3.97112	-4.25026
C	6.398317	-3.13204	-1.33851
H	7.2898	-3.10957	-1.95843
C	-6.77519	-2.72936	-0.8605
H	-7.8189	-2.64752	-1.14951
C	-0.67022	2.739243	-3.40689
H	-0.98866	2.344089	-4.36698
C	-6.32915	-3.85409	-0.16027
H	-7.02685	-4.64726	0.093461
C	-4.44835	1.741508	1.159322
H	-4.54018	2.433569	0.330183
C	-3.13444	0.114458	2.381594
H	-2.20621	-0.43373	2.510066
C	4.698344	-4.36603	-0.15469
H	4.265969	-5.30997	0.164079
C	5.848486	-4.35401	-0.94627
H	6.311613	-5.28663	-1.25311
C	6.579166	2.324878	1.778322
H	7.229494	3.102684	2.166271
C	-4.98706	-3.96051	0.210687
H	-4.63959	-4.83672	0.750254

C	-5.50094	1.553354	2.052271
H	-6.42116	2.114133	1.919384
C	-4.19898	-0.08203	3.260671
H	-4.09749	-0.7929	4.075211
C	-5.38226	0.639757	3.101645
H	-6.20847	0.490173	3.790064

Table S2. The list of the energies of some main frontier energy levels in optimized DPA-PYZ molecule

Electronic orbitals and energies	Electronic cloud distribution
.....
LUMO+2 (-0.93 eV)	
LUMO+1 (-1.04 eV)	
LUMO (-1.92 eV)	
HOMO (-5.30 eV)	
HOMO-1 (-6.18 eV)	
HOMO-2 (-6.54 eV)	
.....

Reference

- 1 a) J. Ge, M. Lan, B. Zhou, W. Liu, L. Guo, H. Wang, Q. Jia, G. Niu, X. Huang, H. Zhou, X. Meng, P. Wang, C. Lee, W. Zhang, X. Han, *Nat. Commun.*, **2014**, *5*, 4596-4604; b) H. Wang, X. Yang, W. Shao, S. Chen, J. Xie, X. Zhang, J. Wang, Y. Xie, *J. Am. Chem. Soc.*, **2015**, *137*, 11376-11382.
- 2 a) Y. Xu, Y. Chen, W. Fu, *Appl. Catal., B*, **2018**, *236*, 176-183; b) C. Xia, R. Fernandes, F. H. Cho, N. Sudhakar, B. Buonacorsi, S. Walker, M. Xu, J. Baugh, L. F. Nazar, *J. Am. Chem. Soc.*, **2016**, *138*, 11219-11226. c) L. Khachatryan, E. Vejerano, S. Lomnicki, B. Dellinger, *Environ. Sci. Technol.*, **2011**, *45*, 8559-8566